Numerical Heat Transfer, vol. 1, pp. 433–451, 1978

FINITE-ELEMENT SOLUTION PROCEDURES FOR SOLVING THE INCOMPRESSIBLE, NAVIER-STOKES EQUATIONS USING EQUAL ORDER VARIABLE INTERPOLATION

G. E. Schneider, G. D. Raithby, and M. M. Yovanovich
Thermal Engineering Group, Department of Mechanical Engineering, University of Waterloo, Waterloo, Ontario, Canada N2L 3G1

The conventional finite-element formulation of the equations of motion (written in pressure-velocity variables) requires that the order of interpolation for pressure be one less than that used for the velocity components. This constraint is inconvenient and can be argued to be physically inconsistent when inertial effects are dominant. The origins of the constraint are discussed and three new finite-element formulations are advanced that permit equal order representation of pressure and velocity. Of these, the velocity correction scheme, similar to that commonly used in finite-difference procedures, offers superior performance for the examples examined in this paper.

INTRODUCTION

The equations governing the steady, viscous flow of an incompressible Stokesian fluid can be written in alternative forms having, respectively, stream function and vorticity, and velocity and pressure (primitive variables), as the dependent variables [1]. The primitive variable formulation (Navier-Stokes equations) consists in two dimensions of the two momentum equations and a zero-velocity-divergence constraint representing mass conservation. When a straightforward finite-element solution is attempted for these problems, a singular matrix is frequently encountered [2]. The standard procedure for avoiding this problem is to reduce the order of the pressure interpolation to one less than that used for the velocity components [3]. Although this is mathematically expedient, the effect of this reduction on solution accuracy has not been clearly established. It has been argued [4] that the reduced order for pressure is, in fact, consistent with the equations of motion, but these arguments are based on a linearization of the acceleration terms in the momentum equations. For the complete nonlinear problem, it would seem that reduced order pressure would be adequate only if viscous effects dominate, but if significant inertial influences are present the pressure field should be interpolated to an equal or even higher order than the velocity.

Several approaches to overcoming the mathematical requirement for reduced order pressure are examined in this paper. These include approaches that employ the Navier-Stokes equations directly and approaches that invoke the incompressibility constraint through the use of a derived equation. Attention is restricted, however, to methods involving the primitive (velocity and pressure) variables explicitly.

The authors thank the National Research Council of Canada for their financial support of this project in the form of operating grants.

0149-5720/78/040433-19$2.75

NOMENCLATURE

A	coefficient matrix [see Eq. (9)]	r	dimensions of component matrices [see Eq. (6)]
b	forcing vector [see Eq. (9)]	Re	Reynolds number ($= LU_p/\nu$)
C_p	specific heat at constant pressure	s	dimensions of component matrices [see Eq. (6)]
D	velocity divergence ($= \partial u_i/\partial x_i$)	t	time
		T	temperature
f^{u_i}, f^p, f^T	forcing vectors for u_i momentum, continuity, and energy, respectively	u_i	velocity component in the x_i direction
		u_p	sliding plate velocity (see Fig. 7)
g_i	component of gravity in the x_i direction	(x, y)	coordinate directions, used interchangeably with (x_1, x_2)
k	thermal conductivity		
$k^{u_i u_i}, k^{pu_i}, \ldots$	coefficients of stiffness matrix [see Eq. (5)]	x_i	coordinate direction, $i = 1, 2$
		∇^2	Laplacian, in two dimensions
L	length scale (see Figs. 3 and 7)	μ	dynamic viscosity
m	matrix dimensions [see Eq. (7)]	ρ	fluid density
		ϕ	velocity-correction potential [see Eq. (18)]
n	matrix dimensions [see Eq. (7)]		
		λ	eigenvalue [see Eq. (10)]
N	shape functions [see Eq. (9)]	β	isobaric compressibility
P	pressure	δ	artificial compressibility
Pr	Prandtl number [see Eq. (24)]	ν	kinematic viscosity
Ra	Rayleigh number [see Eq. (25)]	α	thermal diffusivity

An artificial compressibility method, employing the Navier-Stokes equations directly, is examined with respect to its potential for surmounting the pressure interpolation problem. Results presented for this method support the eigenvalue analysis reported in [5].

The use of the pressure Poisson equation as a mechanism for invoking the incompressibility constraint is also investigated in this work. The pressure Poisson equation is a derived equation for pressure (obtained from the momentum equations) that replaces the zero-divergence continuity constraint. Previous attempts to use this equation in a prediction scheme have met with failure [6] and partial success [5]. Additional experience with this method is gained in this work.

The relatively poor performance of the pressure Poisson methods as previously applied [5, 6] has led us to reexamine this equation with respect to its predictive capabilities in a computational method. The details of this reexamination of the pressure Poisson equation are reported in [7]. In that paper a partial explanation was provided for the relatively poor performance of the method and a new method based on the pressure Poisson equation was proposed. The proposed method provides a significant improvement over the previous methods involving the pressure Poisson equation, but computationally undesirable features remain and are thought to result from the indirect manner in which the incompressibility constraint is enforced.

Finally, an alternative method is presented to the finite-element community having as its basis the stringent satisfaction of continuity at every stage of the iterative approach toward a converged solution. This method, the velocity correction procedure, is modeled after a method employed by finite-difference researchers [8] and, of the

methods examined in this paper, it is felt to provide the most promise where equality of representation of the velocity and pressure fields is demanded of the procedure. Experience with this method indicates that an order of magnitude reduction in computational cost can be achieved over other methods that will permit the above equality of representation.

These methods are applied to three example problems to assist in evaluating the relative potential of the methods for surmounting the reduced order pressure interpolation requirement.

OUTLINE OF FINITE-ELEMENT FORMULATION

Consider the two-dimensional flow of a Stokesian fluid having constant properties. The governing differential equations are given by [9]

$$\rho \frac{\partial u_i}{\partial t} + \rho u_j \frac{\partial u_i}{\partial x_j} = -\frac{\partial P}{\partial x_i} + \mu \nabla^2 u_i + \rho g_i \qquad i, j = 1, 2 \tag{1}$$

and

$$\frac{\partial u_i}{\partial x_i} = 0 \tag{2}$$

where u_i denotes the velocity component in the x_i direction, ρ is the fluid density, P is pressure, g_i is the component of gravitational acceleration in the x_i direction, and ∇^2 is the Laplacian operator in two dimensions. The equation for conservation of thermal energy, neglecting compression work and viscous dissipation, is given by

$$\rho C_p \frac{\partial T}{\partial t} + \rho C_p u_j \frac{\partial T}{\partial x_j} = k \nabla^2 T \tag{3}$$

where T is temperature, C_p is the fluid specific heat, and k is the fluid thermal conductivity. Equations (1)-(3) represent four equations in the four unknowns, u_1, u_2, P, and T. A method of solution of this set of equations is sought.

In the finite-element method, the unknown velocity, pressure, and temperature fields are expressed in terms of interpolation formulas over each element of the subdivided domain. This is readily accomplished through the use of shape functions N [10], and the approximate solution fields then take the form

$$\begin{aligned} u_i &= \{N_k{}^{u_i}\}^T \{u_{i_k}\} \\ P &= \{N_k{}^{P}\}^T \{p_k\} \\ T &= \{N_k{}^{T}\}^T \{T_k\} \end{aligned} \tag{4}$$

By adopting the Galerkin method of error distribution, the residuals obtained through substitution of Eqs. (4) into the governing differential equations (1)-(3) are weighted using the shape functions for the velocity components, pressure, and temperature, respectively, and the volume-integrated result is set to zero. Equations (1)

and (3) are nonlinear and a suitable linearization is therefore required. The linearization utilized herein consists of approximating the "convecting" velocities of Eqs. (1) and (3) by suitable guess distributions. Details regarding the linearization procedure can be found in [3] and [11]. By employing backward differences in time, the finite-element equations can be written in matrix form as

$$\begin{bmatrix} [K^{u_1u_1}] & 0 & [K^{u_1p}] & 0 \\ 0 & [K^{u_2u_2}] & [K^{u_2p}] & 0 \\ [K^{pu_1}] & [K^{pu_2}] & 0 & 0 \\ 0 & 0 & 0 & [K^{TT}] \end{bmatrix} \begin{bmatrix} \{u_1\} \\ \{u_2\} \\ \{p\} \\ \{T\} \end{bmatrix} = \begin{bmatrix} \{f^{u_1}\} \\ \{f^{u_2}\} \\ \{f^p\} \\ \{f^T\} \end{bmatrix} \tag{5}$$

Details regarding the evaluation of the component entries in this system of equations can be found in [11].

THE PRESSURE INTERPOLATION PROBLEM

The pressure interpolation problem arises when the set of algebraic equations represented in Eq. (5) is modified to incorporate boundary conditions. This will be demonstrated by asserting Dirichlet conditions on the momentum-continuity subset of equations.

The equation formed by weighting one of the momentum equations by the kth shape function for velocity can be considered to be an equation expressing momentum conservation in this direction in the vicinity of the kth velocity node of the discrete system. The equation formed by weighting the continuity equation by the kth shape function for pressure can be considered to be an equation expressing the conservation of mass (for incompressible fluids the compression work done by the pressure field must be zero) in the vicinity of the kth pressure node. With this view, the momentum equations are considered as equations for the nodal velocity components and the continuity equations are considered as equations for the nodal pressures.

The procedure for invoking specified velocity boundary values is to delete (or not form) the appropriate equation describing momentum conservation in favor of the boundary velocity value specification. For specified pressures the appropriate continuity equation is deleted in favor of the boundary pressure specification. Support for this procedure of boundary condition specification is provided in [2, 3, 11, 12]. The impact that adoption of the above procedure has on the pressure interpolation problem will now be discussed.

The number of nodal velocities and pressures required is determined in direct relation to the interpolation order used to define the approximate velocity and pressure fields, respectively. In what follows it will be assumed that the compatibility and completeness requirements of the shape functions have been met and moreover, to maintain geometric isotropy, that the shape functions used for the two velocity components are equal.

By letting r denote the number of velocity nodes and s the number of pressure nodes, the matrix equation (5) can be written for the present problem, prior to boundary condition application, as

$$\begin{bmatrix} [K^{u_1u_1}]_{rxr} & 0 & [K^{u_1p}]_{rxs} \\ 0 & [K^{u_2u_2}]_{rxr} & [K^{u_2p}]_{rxs} \\ [K^{pu_1}]_{sxr} & [K^{pu_2}]_{sxr} & 0 \end{bmatrix} \begin{bmatrix} \{u_1\} \\ \{u_2\} \\ \{p\} \end{bmatrix} = \begin{bmatrix} \{f^{u_1}\} \\ \{f^{u_2}\} \\ 0 \end{bmatrix} \tag{6}$$

Further, by denoting the number of velocity-specified nodes by e and the number of pressure-specified nodes by f, the number of velocity equations requiring solution will be $m \equiv r - e$ for each component, and the number of continuity (pressure) equations requiring solution will be $n \equiv s - f$. The resulting system of matrix equations requiring solution can then be written as

$$\begin{bmatrix} [K^{u_1u_1}]_{mxm} & 0 & [K^{u_1p}]_{mxn} \\ 0 & [K^{u_2u_2}]_{mxm} & [K^{u_2p}]_{mxn} \\ [K^{pu_1}]_{nxm} & [K^{pu_2}]_{nxm} & 0 \end{bmatrix} \begin{bmatrix} \{u_1\} \\ \{u_2\} \\ \{p\} \end{bmatrix} = \begin{bmatrix} \{f^{u_1}\} \\ \{f^{u_2}\} \\ 0 \end{bmatrix} \tag{7}$$

In order that the overall system admit a solution, the conditions must be met that

$$m + n \geqslant m \quad (x \text{ momentum}) \tag{8a}$$

$$m + n \geqslant m \quad (y \text{ momentum}) \tag{8b}$$

$$2m \geqslant n \quad (\text{continuity}) \tag{8c}$$

It is from the above conditions that the shape function restriction for pressure interpolation can be seen. While satisfaction of the first two criteria is trivial, violation of the third is clearly possible. This is particularly true if the velocity and pressure shape functions are of the same polynomial degree.

In the report by Tuann and Olson [13] an alternative viewpoint is presented on the pressure interpolation problem, which also hinges on the application of boundary conditions. Writing Eq. (6) in the form

$$[A]\{x\} = \{b\} \tag{9}$$

they recognized that the solutions to the eigenvalue problem defined by

$$[[A] - \lambda[I]]\{x\} = \{0\} \tag{10}$$

and for which the eigenvalues are zero, constitute solutions to the homogeneous form of Eq. (9). The associated modal vectors must therefore be suppressed or accepted through the application of boundary conditions. It was shown that if insufficient pressure information was given, spurious pressure solutions would persist in the solution field. A sufficiently stringent specification of the pressure boundary values may not be possible, however, with the boundary data available for a given problem.

ARTIFICIAL COMPRESSIBILITY SCHEME

The difficulty encountered above is a result of pressure failing to appear explicitly in the continuity equation, and this, in turn, is a result of the assumed independence of the density on the pressure field for incompressible fluids.

By restricting attention to steady flows, the problem could be avoided if an equation of state were employed that related density to pressure such that the continuity equation would explicitly contain pressure. In the artificial compressibility scheme, an artificial density is introduced that exhibits this dependence on pressure. This artificial density is introduced only in the continuity equation and is structured such that the steady solution will be unaffected. These ideas will be clarified in the following discussion.

A computational method based on these ideas was originally proposed by Chorin [14] for use in finite-difference computation. In this method the artificial equation of state relating the fictitious density ρ^* to pressure is

$$\rho^* = P\delta \tag{11}$$

where δ is an artificial compressibility. Further, the fictitious density is introduced only in the temporal term of the continuity equation. The continuity equation is then written as

$$\delta \frac{\partial P}{\partial t} + \frac{\partial u_i}{\partial x_i} = 0 \tag{12}$$

in which the pressure now appears explicitly.

Use of the above equation admits a physical interpretation of the computational process in which the velocity divergence is driven to zero as steady state is approached and temporal variations vanish. The mechanism is to provide a pressure increase (decrease) in regions of local negative (positive) divergence. Thus, mass sources tend to be annihilated through the local pressure decrease, which acts through the momentum equations to drive less mass out of these regions.

A finite-element representation of Eq. (12) can be readily derived by employing standard methods and will not be presented here. Instead, attention is directed to the application of the method to the example of pressure-driven flow between stationary plates. The problem geometry and boundary conditions are illustrated in Fig. 1. On the two horizontal boundaries a zero-slip condition is applied. Further, since the procedure follows a transient-like development, a pressure datum is not supplied, but the pressure is left to seek its own level starting from an initial field of zero. The flow Reynolds number based on plate spacing was of order unity. Isoparametric, quadratic, quadrilateral elements were used in the finite-element discretization (equal order for velocity and pressure).

Two possible procedures can be adopted for application of the method: a simultaneous solution of the momentum and continuity equations, or an iterative approach that involves alternately solving the momentum equations for the velocity components and the continuity equation for pressure. Because of the corrective nature of the procedure as described above, the simultaneous solution approach proved

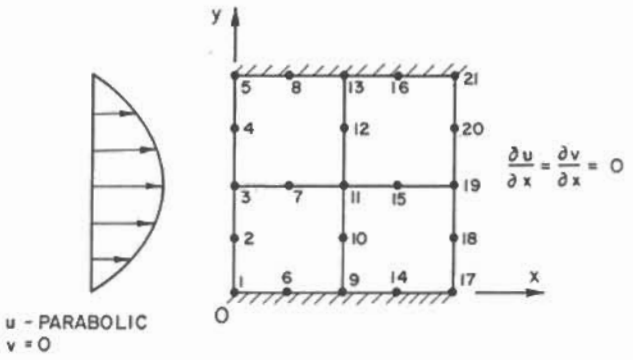

Fig. 1 Problem geometry used for Couette flow example.

unsuccessful in providing convergent solutions, although a singular matrix (i.e., the "pressure interpolation problem") was never encountered. Thus, the objective of overcoming the singular matrix problem has been achieved.

Adopting the iterative approach to the artificial compressibility scheme permitted convergent solutions to this problem to be obtained. A dimensionless time step of $\nu \Delta t/L^2 = 50$, where ν is the kinematic viscosity, Δt the time interval, and L the plate spacing, was found to provide stable solutions over a wide range of the artificial compressibility. A near-optimal value of the compressibility was found to be $\delta \approx 1.5$ for the Reynolds number under consideration.

With the pressure interpolation problem surmounted, attention is now directed to solution accuracy. It was observed that the velocity field agreement with the exact solution for this problem was excellent. However, the pressure field exhibited quadratic "bumps" in both dimensions of the computational domain, although the average overall pressure drop was approximately correct. This result is indeed disturbing, that such an unusual pressure field is actually compatible with the finite-element representation of the equations of motion.

Despite the inaccurate prediction of the pressure field as indicated above, the artificial compressibility study has served a very useful purpose. The above results provide quantitative substantiation of the eigenvalue analysis predictions of Tuann and Olson [13]. In their analysis, they predicted that where quadratic interpolation for velocity and pressure is used, quadratic spurious solutions in the pressure field could persist in the numerical predictions. Our experience completely confirms these predictions.

Because of the inability of the method to provide accurate pressure solutions, in addition to several other detrimental features of the method as detailed in Schneider [11], the artificial compressibility scheme is discarded as a viable means for the finite-element prediction of incompressible fluid flows where equality of the velocity and pressure interpolation is demanded of the solution.

PRESSURE POISSON FORMULATION

An alternate approach to overcoming the pressure interpolation problem by utilizing the pressure Poisson equation is discussed in [7]. This offers the potential for

overcoming the problems associated with the weak coupling between the pressure and velocity fields by placing pressure in a more dominant role. The equation is derived by taking the divergence of the vector momentum equation and is given by

$$\nabla^2 P = 2\rho\left[\frac{\partial u_1}{\partial x_1}\frac{\partial u_2}{\partial x_2} - \frac{\partial u_2}{\partial x_1}\frac{\partial u_1}{\partial x_2} - \frac{D^2}{2}\right] + \left\{\mu\nabla^2 D - \rho u_j \frac{\partial D}{\partial x_j} - \rho\frac{\partial D}{\partial t}\right\} + \frac{\partial(\rho g_j)}{\partial x_j} \quad (13)$$

where

$$D \equiv \frac{\partial u_j}{\partial x_j} \quad (14)$$

is the velocity field divergence and μ is the dynamic viscosity. Invoking the incompressible continuity equation that $D = 0$ everywhere in the solution domain results in the simplified pressure Poisson equation

$$\nabla^2 P = 2\rho\left[\frac{\partial u_1}{\partial x_1}\frac{\partial u_2}{\partial x_2} - \frac{\partial u_2}{\partial x_1}\frac{\partial u_1}{\partial x_2}\right] + \frac{\partial(\rho g_j)}{\partial x_j} \quad (15)$$

As discussed in [7], the mathematical problem then becomes that of solving the two momentum equations in harmony with Eq. (15).

A finite-element representation can be readily derived for the above Poisson equations and will not be presented here. It is noted, however, that boundary conditions are required for the pressure and that the appropriate conditions are those of self-consistency. That is, pressure gradients at the boundary are made consistent with those obtained from the momentum equations. A datum for pressure is also required if there are no pressure-specified boundaries in the problem.

Decisions must be made at this point regarding the mode of application of this formulation. Previous efforts [6, 13] in this direction have employed approaches that are completely iterative in their nature, the momentum and pressure Poisson equations being solved successively in sequence. We solved these equations simultaneously for velocity and pressure with the coupling of the pressure Poisson equation to the momentum equations provided through the boundary self-consistency conditions.

The procedure described above was applied to the Couette flow problem illustrated in Fig. 1 for the boundary conditions indicated in that figure as well as for several other boundary condition combinations consistent with the well-posed Navier-Stokes problem. It was concluded, on the basis of this experience, that the formulation performed very well for this example. Solutions were obtained with equal order pressure and velocity interpolation, and these solutions were free from the undesirable features of the artificial compressibility solutions. A second, more demanding problem is now examined.

The second example considered is that of free convection flow within a square enclosure. The geometry and boundary conditions are indicated in Fig. 2. A Boussinesq approximation is made, that density variations are considered only where they appear in the momentum equations as driving forces. The no-slip condition is applied at all boundaries, and a reference pressure of zero is assumed at the midcavity node. The flow field is characterized by the Prandtl and Rayleigh numbers (Eckert and Drake

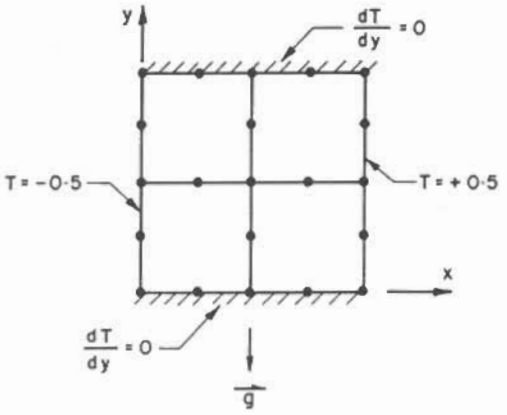

Fig. 2 Problem geometry used for free convection example.

[15]), Pr and Ra, where Pr = 0.73 for air was used in all computations. Quadratic, isoparametric, quadrilateral finite elements were again used for all variables.

Initial experiments with Ra = 0 verified the no-flow situation; the Rayleigh number was then increased. The initial velocity and pressure fields were zero with the temperature linearly varying from the hot surface to the cold surface. For a Rayleigh number of 250, a relatively slow recirculation situation, a converged solution was achieved in 5 Picard iterations, convergence corresponding to a maximum change in any variable of less than 0.1% between successive iterations. With an advanced Rayleigh number of 1000, a converged solution was also obtained but significantly more iterations were required. For the further increased Rayleigh number of 10,000, a converged solution could not be obtained within practical computing times despite many attempts.

The failure to yield a solution to this problem provided the incentive to undertake a separate investigation of the pressure Poisson formulation [7]. The reasons why poor performance can be expected from this formulation and the reasons for the failure in this problem are discussed in detail in [7]. A similar formulation, but with much improved convergence characteristics, was also presented, which permitted a solution to the natural convection problem to be obtained for a Rayleigh number of 10,000. Although this success supported the arguments for the failure of the pressure Poisson formulation, the procedure was not extensively tested because of the even better performance of the formulation described in the following section.

THE VELOCITY CORRECTION PROCEDURE

The experience mentioned above and that of finite-difference researchers suggest that conservation of mass is of paramount importance in computing fluid flows. The velocity correction procedure is based on the ideas of Chorin [16], Amsden and Harlow [17], and Patankar [18], and provides a more direct enforcement of mass conservation than the previously discussed method. The velocity correction procedure is now described.

A tentative velocity field u_1^* and u_2^* is obtained from the momentum equations under the influence of a guessed pressure field p^*. These velocities will not, in general, satisfy mass conservation, and corrections are introduced in the usual form

$$u_i = u_i^* + u_i' \qquad i = 1, 2 \tag{16}$$

The continuity equation can then be written solely in terms of the velocity correction field as

$$\frac{\partial u_i'}{\partial x_i} = -D^* \tag{17}$$

In recognition that the pressure field cannot alter the vorticity of the flow, the correction field will be obtained in such a way that (1) it leaves the vorticity of the u_i^* field unchanged, and (2) the incompressibility constraint, Eq. (17), will be satisfied. These requirements can be fulfilled if the velocity correction is defined to be the gradient of a suitable potential function ϕ. Thus the definition is made that

$$u_i' \equiv \frac{\partial \phi}{\partial x_i} \qquad i = 1, 2 \tag{18}$$

With this definition, Eq. (17) becomes

$$\nabla^2 \phi = -D^* \tag{19}$$

The solution of this equation will permit the velocity correction field to be determined that, when added to the u_i^* field, will produce a velocity field satisfying conservation of mass exactly. (Conservation of momentum, however, will not be satisfied by the resultant field.) The final step of the iterative cycle consists of obtaining a more realistic estimate of the pressure distribution than that used at the beginning of the cycle. This is done using the pressure Poisson equation in the form of Eq. (15).

The velocity correction procedure is not as directly implemented as the description above might suggest. The problem arises in providing realistic boundary conditions for the u_i^* field, for these are not known a priori. The true physical boundary conditions can be applied to the u_i^* field with the view that, as the correction potential ϕ vanishes, the steady solution will be unaffected, or a more elaborate procedure as discussed in Schneider et al. [7] can be adopted. Fortunately, the former approach appears to provide satisfactory convergence characteristics based on experience with the problems on which it has been applied to date.

The velocity correction procedure was applied to the free convection problem and extremely rapid convergence, relative to that realized using the previous methods, was observed. Relatively large time steps were permissible even for the case where Ra = 10,000. The solutions were obtained using isoparametric, quadratic, quadrilateral elements for both the pressure and velocity fields. The success of the method, as further evidenced by the applications discussed below, is attributed to the strong, direct enforcement of the incompressibility constraint. Convergence rates an order of magnitude faster than those of the best pressure Poisson formulation were observed.

PREDICTIONS FROM THE VELOCITY CORRECTION PROCEDURE

The velocity correction procedure has been applied to two problems in order to obtain a preliminary evaluation of the impact that equality of representation of the velocity and pressure fields has on the computed results. These applications are now discussed.

Free Convection in an Enclosed Cavity

The first problem is similar to the free convection example already considered with the exception that the horizontal sidewalls are assigned a linear temperature distribution corresponding to infinitely conducting sidewalls. The problem geometry and boundary conditions are illustrated in Fig. 3.

The differential equations governing the flow in the cavity are

$$\frac{\partial u_i^*}{\partial t^*} + u_j^* \frac{\partial u_j^*}{\partial x_j^*} = -\frac{\partial P^*}{\partial x_i^*} + \mathrm{Pr}\,\nabla^2 u_i^* + \mathrm{Ra}\,\mathrm{Pr}\frac{g_i}{g} T^* \tag{20}$$

$$\frac{\partial u_j^*}{\partial x_j^*} = 0 \tag{21}$$

and

$$\frac{\partial T^*}{\partial t^*} + u_j^* \frac{\partial T^*}{\partial x_j^*} = \nabla^2 T^* \tag{22}$$

where the nondimensional variables are defined by

$$\begin{aligned} x_i^* &= \frac{x_i}{L} \qquad u_i^* = \frac{u_i}{u_0} \\ t^* &= \frac{\alpha t}{L^2} \qquad p^* = \frac{p}{\rho {u_0}^2} \\ T^* &= \frac{1}{2} - \frac{T_h - T}{T_h - T_c} \end{aligned} \tag{23}$$

with $u_0 = \alpha/L$, where α is the thermal diffusivity, and T_h and T_c are the hot and cold boundary temperatures, respectively. The Prandtl and Rayleigh numbers are defined, respectively, by

$$\mathrm{Pr} \equiv \frac{\nu}{\alpha} \tag{24}$$

and

$$\mathrm{Ra} \equiv \frac{\beta_p (T_h - T_c) g L^3}{\nu \alpha} \tag{25}$$

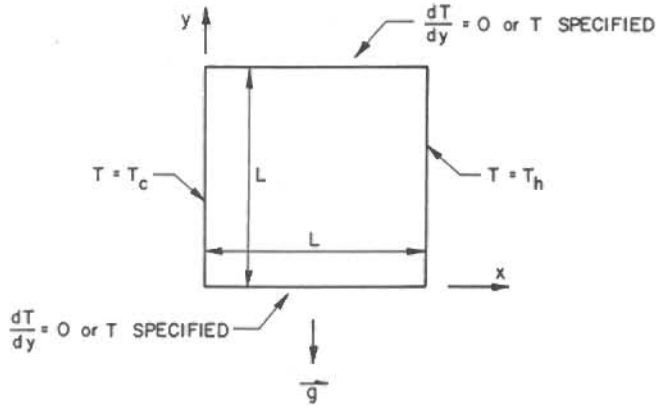

Fig. 3 Problem geometry used for free convection example.

where β_p is the isobaric compressibility and g is the gravitational acceleration. Boundary conditions are self-evident from the text description and will not be displayed in their mathematical form. Boundary conditions for the pressure Poisson equation are the self-consistency conditions described earlier.

A solution was obtained to the above problem for a Rayleigh number of 100,000. A Prandtl number of 0.73 was used, corresponding to air at approximately standard temperature and pressure conditions. Although computational expediency can be realized through the use of nonuniform meshes, a uniform subdivision was used for the demonstrative purposes intended of the examples. Quadratic, isoparametric quadrilateral finite elements were used.

Velocity profiles computed for the Ra = 100,000 problem are presented in Fig. 4, using a mesh of 8 elements by 8 elements. It is noted that in the reentrant corners (lower right and upper left), a discontinuity in the vertical velocity component gradient is incurred. This was not observed for the Ra = 10,000 problem (at the same discretization level) and is attributed to the boundary-layer character of the flow

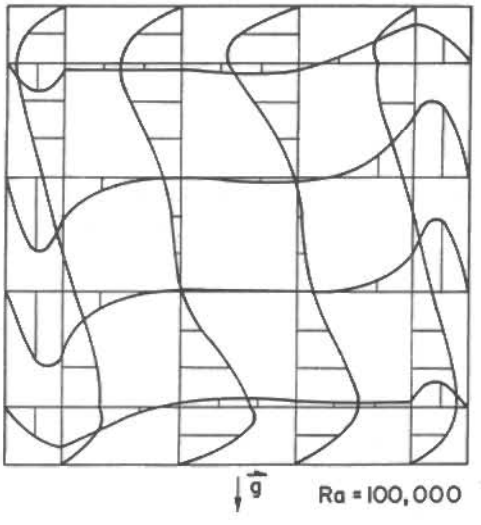

Fig. 4 Velocity profiles computed for the free convection example for Ra = 100,000, using an 8 × 8 mesh.

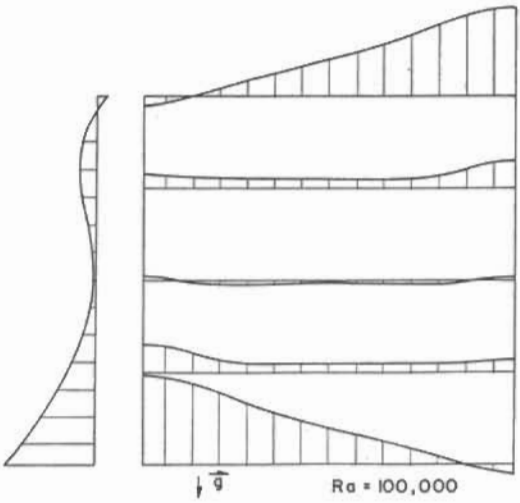

Fig. 5 Pressure profiles computed for the free convection example for Ra = 100,000, using an 8 × 8 mesh and quadratic pressure interpolation.

resulting from the high concentration of buoyancy influences in these regions at this high Rayleigh number. The flow trends are well represented, however, and it is noted that the above-mentioned discontinuities are also experienced when the conventional approach with reduced order pressure interpolation is employed.

The computed pressure distribution is illustrated in Fig. 5 for this problem. The quadratic pressure interpolation is seen to provide a smooth and continuous representation of the pressure field. Although the quadratic capability does not appear necessary to describe the horizontal pressure variation, there are definite quadratic variations exhibited in the vertical pressure distribution. In contrast to the above, solutions obtained employing a linear pressure interpolation are presented in Fig. 6 for a 7 X 7 mesh.

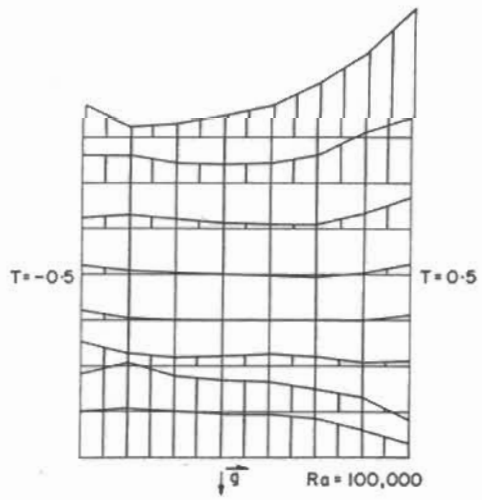

Fig. 6 Pressure profiles computed for the free convection example for Ra = 100,000, using a 7 × 7 mesh and linear pressure interpolation.

It is clear from examination of Figs. 5 and 6 that the linear pressure results experience difficulty in smoothly describing the pressure field, while the quadratic results provide a smoothly varying pressure field. This suggests that there may be an increase in the pressure distribution accuracy obtained through the use of equal order pressure and velocity interpolation, although detailed predictions or observations of the pressure field are not available in the literature for this problem. The velocity field, however, differs only slightly from that obtained using the conventional finite-element method.

Shear Driven Flow in a Cavity

The second problem examined using the velocity correction procedure is the so-called driven cavity problem—that of shear driven flow in a cavity, one sidewall of which is moving at constant and uniform velocity. The problem geometry is illustrated in Fig. 7 for a square cavity. No-slip boundary conditions are prescribed for the velocity components over the cavity boundary with nonzero velocity applied to the rightmost wall. Two values of the Reynolds number $\mathrm{Re} \equiv u_p L/\nu$ were considered, $\mathrm{Re} = 100$ and $\mathrm{Re} = 400$, where u_p is the velocity of the rightmost boundary.

The governing differential equations for this problem are

$$\frac{\partial u_i^*}{\partial t^*} + u_j^* \frac{\partial u_i^*}{\partial x_j^*} = -\frac{\partial P^*}{\partial x_i^*} + \nabla^2 u_i^* \tag{26}$$

and

$$\frac{\partial u_j^*}{\partial x_j^*} = 0 \tag{27}$$

where the nondimensional variables are

$$x_i^* = \frac{x_i}{L} \quad u_i^* = \frac{u_i}{u_p} \quad t^* = \frac{\nu t}{L} \quad p^* = \frac{p}{\rho u_p{}^2} \tag{28}$$

The nonhomogeneous boundary condition applies to the rightmost boundary and is given by $u_2^*(x_1^* = 1) = -\mathrm{Re}$. The singularities at the moving boundary corners were handled by prescribing a transition profile over a thin element adjacent to the moving

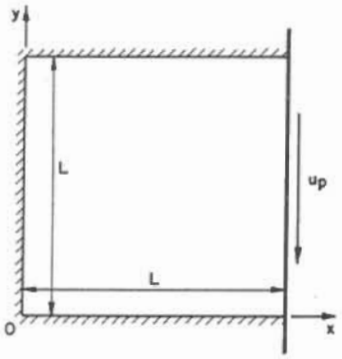

Fig. 7 Problem geometry for the driven cavity example.

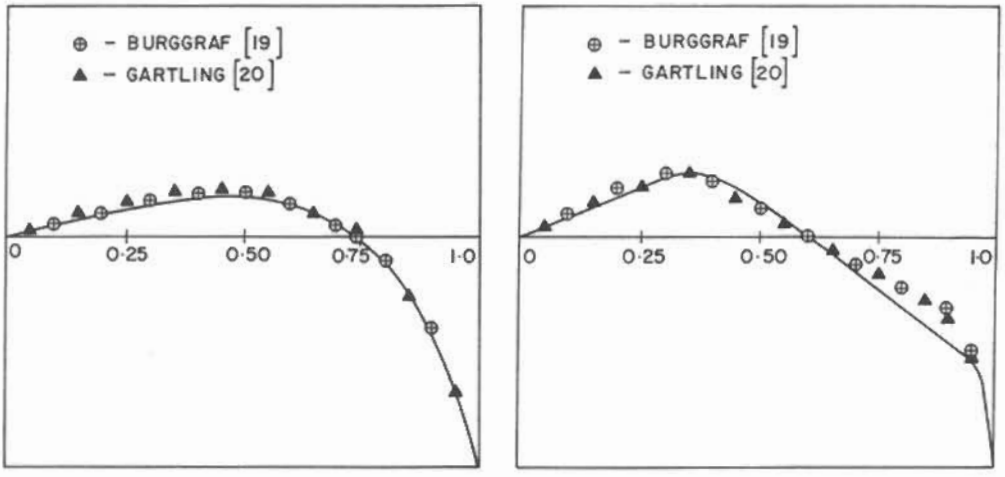

Fig. 8 Comparison of cavity centerline vertical velocity profiles with the results of Gartling and Burggraf for (*a*) Re = 100 and (*b*) Re = 400.

boundary. The transition profile for u_2^* was selected such that the velocity gradient at the interfaces between the thin elements and the internal elements vanished at the upper and lower cavity boundaries.

Solutions were obtained by impulsively starting the lid in motion at time $t = 0$. Quadratic, isoparametric, quadrilateral elements were used with seven elements in the x_1 direction (including the thin row) and five elements in the x_2 direction. As a basis for solution verification, the u_2 velocity profile along the horizontal cavity centerline will be used as presented by Burggraf [19] and Gartling [20]. This velocity profile is shown in Fig. 8, *a* and *b*, for the Re = 100 and 400 cases, respectively. The solid line represents the present predictions and it can be seen that agreement with the solution of Burggraf and Gartling is generally good. Although linear pressure interpolation solutions were also obtained for these problems, the velocity profiles differed only slightly from those presented in Fig. 8. The quadratic and linear interpolation pressure solutions showed a substantially larger difference. For the Re = 100 case, the quadratic and linear pressure solutions are shown in Fig. 9. It can be seen from Fig. 9 that the quadratic pressure solutions agree quite well with Burggraf's predictions (he used a 51 X 51 finite-difference mesh), while the linear pressure results indicate a significant departure from the Burggraf numerical data. The pressure fields for quadratic and linear pressure interpolation for the Re = 400 problem are presented in Fig. 10, *a* and *b*, respectively. Again, the quadratic pressure interpolation results are in significantly better agreement with the Burggraf results than are the linear pressure results.

It is noted that, although the velocity predictions are relatively insensitive to inaccuracies in the pressure solution, the accuracy of the pressure field itself is significantly affected by the pressure interpolation order. Thus, where pressure field accuracy is required, the velocity correction procedure offers the capability of providing increased pressure accuracy by permitting equal order velocity and pressure interpolation to be used.

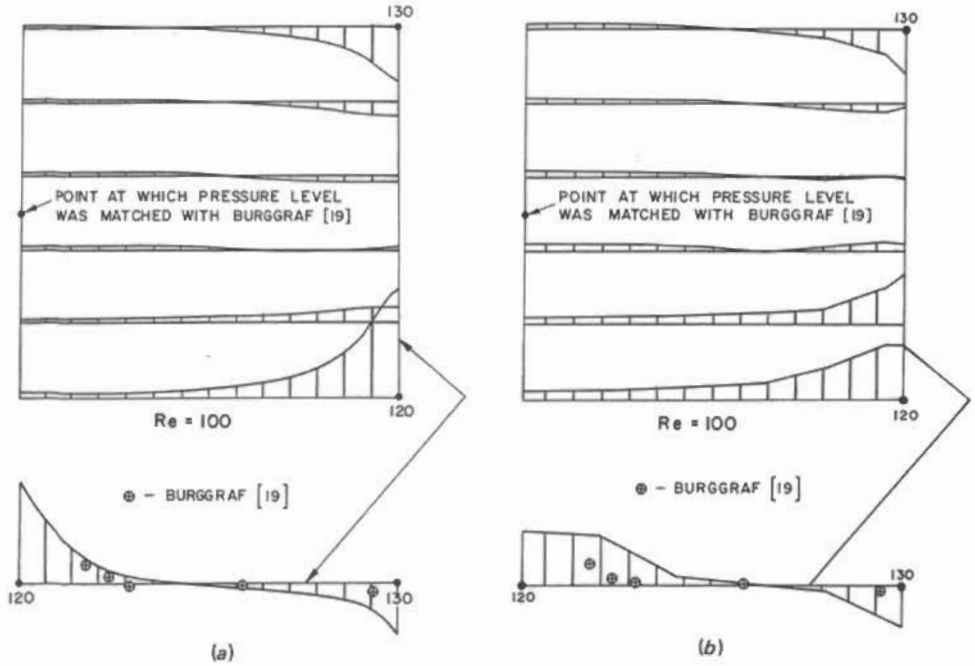

Fig. 9 Pressure profiles computed for the driven cavity example for Re = 100 using (*a*) quadratic pressure interpolation and (*b*) linear pressure interpolation.

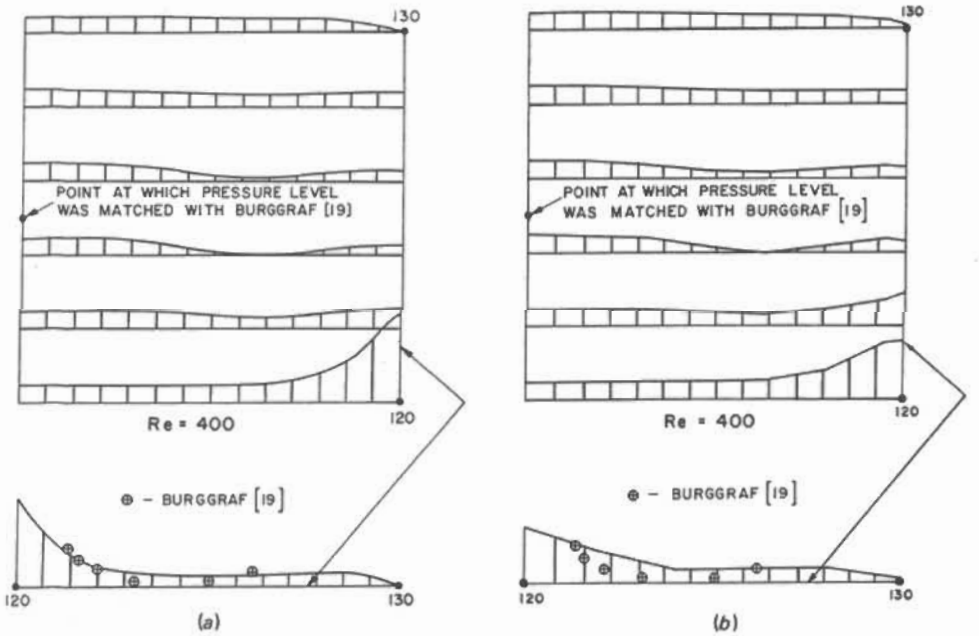

Fig. 10 Pressure profiles computer for the driven cavity example for Re = 400 using (*a*) quadratic pressure interpolation and (*b*) linear pressure interpolation.

DISCUSSION AND CONCLUSIONS

The objective of the research program described in this paper has been the removal of the requirement that the pressure field interpolation be of a lower order than the velocity interpolation in the finite-element solution of fluid flow problems. To this end, several methods have been proposed and examined, and to varying degrees these have been successful in surmounting this obstacle. Definitive answers regarding the *accuracy* of the proposed methods have not been provided in this paper, but this question is beyond the scope of the current study. Much additional work will be required to provide these answers. However, the groundwork has been laid in this paper to indicate the directions that this future research can take.

It was demonstrated early in the paper how singular matrix equations may result when equality of pressure and velocity representation is demanded of the conventional finite-element formulation. The emergence of singular matrix equations was shown to be linked to the application of boundary conditions to the algebraic equations.

The artificial compressibility scheme has been introduced in this paper to the finite-element community, and this method was successful in surmounting the singular matrix problem. The undesirable features accompanying the use of this method, however, make this approach inadequate for use in fluid flow computation. The application of the method, however, has served to confirm the eigenvalue predictions of Tuann and Olson [13].

Two pressure Poisson formulations were employed in this work and both proved successful in surmounting the pressure interpolation problem. The first form of the method was found to yield intolerably slow convergence rates on problems in which the recirculation rate is high. The second form of the method, wherein the Poisson equation is used more appropriately for the determination of a pressure correction field, provided a significant improvement over the first form of the method.

The velocity correction procedure has been introduced to finite-element analysis of fluid flow and provides the first viable computational method for solving problems with equality of representation of the pressure and velocity fields. Its success has been attributed to the strict enforcement of the continuity constraint at every stage of the iterative process. An order of magnitude increase in the convergence rate over the previous methods was observed for the free convection problem at a Rayleigh number of 10,000.

A preliminary assessment of the influence that reduced order pressure may have on solution accuracy was made by way of two examples: the perfectly conducting sidewall case of the free convection problem at a Rayleigh number of 100,000, and the driven cavity problem at Reynolds numbers of 100 and 400. Qualitatively and quantitatively correct velocity solutions were obtained in both cases. Although these computed velocity distributions were observed to be insensitive to the pressure interpolation order, the computed pressure distributions were highly sensitive to the order of interpolation. The experience gained on the driven cavity problem indicates that a significant improvement in pressure solution accuracy can be obtained using an equal order pressure and velocity representation.

Although the efforts described in this paper, and in particular the examples considered, deal with equality of representation of the pressure and velocity field interpolation, the original impetus for the work was the removal of the restriction that

the pressure interpolation be of a lower order than that used for velocity. Consequently, the arguments presented here also apply to the use of pressure interpolation that is higher in order than that used for the velocity field, and this may be desirable in certain situations. Explicit consideration has not been given, however, to a higher order pressure method.

REFERENCES

1. C. Taylor and P. Hood, A Numerical Solution of the Navier-Stokes Equations Using Finite Element Technique, *Comput. Fluids*, vol. 1, no. 1, pp. 73–100, 1973.
2. Y. Yamada, K. Ito, Y. Yocouchi, T. Tamano, and T. Ohteubo, Finite Element Analysis of Steady Fluid and Metal Flow, in R. H. Gallagher, J. T. Oden, C. Taylor, and O. C. Zienkiewicz (eds.), *Finite Elements in Fluids*, vol. 1, pp. 73–94, Wiley, New York, 1975.
3. K. H. Huebner, *The Finite Element Method for Engineers*, Wiley, New York, 1975.
4. P. Hood and C. Taylor, Navier-Stokes Equations Using Mixed Interpolation, in J. T. Oden, O. C. Zienkiewicz, R. H. Gallagher, and C. Taylor (eds.), *Finite Element Methods in Flow Problems*, pp. 121–132, Univ. of Alabama Press, Huntsville, Ala., 1974.
5. M. D. Olson and S. Y. Tuann, Primitive Variables Versus Stream Function Finite Element Solutions of the Navier-Stokes Equations, presented at the Second International Symposium on Finite Element Methods in Flow Problems, Santa Margherita Ligure, Italy, June 1976.
6. P. Hood, A Finite Element Solution of the Navier-Stokes Equations for Incompressible Contained Flow, M.Sc. thesis, Univ. of Wales, Swansea, 1970.
7. G. E. Schneider, G. D. Raithby, and M. M. Yovanovich, Finite Element Analysis of Incompressible Fluid Flow Incorporating Equal Order Pressure and Velocity Interpolation, presented at the International Conference on Numerical Methods in Laminar and Turbulent Flow, Swansea, Wales, July 18–21, 1978.
8. F. H. Harlow and J. E. Welch, Numerical Calculation of Time Dependent Viscous Incompressible Flow of Fluid with Free Surface, *Phys. Fluids*, vol. 8, no. 12, p. 2182–2189, 1965.
9. R. B. Bird, W. E. Stewart, and E. N. Lightfoot, *Transport Phenomena*, Wiley, New York, 1960.
10. O. C. Zienkiewicz, *The Finite Element Method in Engineering Science*, McGraw-Hill, New York, 1971.
11. G. E. Schneider, Finite Element Analysis of Incompressible Fluid Flow Incorporating Equal Order Pressure and Velocity Interpolation, Ph.D. thesis, Univ. of Waterloo, Ontario, Canada, 1977.
12. J. T. Oden and L. C. Wellford, Jr., Analysis of Flow of Viscous Fluids by the Finite Element Method, *AIAA J.*, vol. 10, no. 12, pp. 1590–1599, 1972.
13. S. Y. Tuann and M. D. Olson, A Study of Various Finite Element Solution Methods for the Navier-Stokes Equations, *Struct. Res. Ser. Rept. 14*, Dept. of Civil Engineering, Univ. of British Columbia, Vancouver, May 1976.
14. A. J. Chorin, A Numerical Method for Solving Incompressible Viscous Flow Problems, *J. Comput. Phys.*, vol. 2, pp. 12–16, 1967.
15. E. R. G. Eckert and R. M. Drake, Jr., *Analysis of Heat and Mass Transfer*, McGraw-Hill, New York, 1972.
16. A. J. Chorin, Numerical Solution of the Navier-Stokes Equations, *Math. Comput.*, vol. 22, pp. 745–762, 1968.

17. A. A. Amsden and F. H. Harlow, The SMAC Method: A Numerical Technique for Calculating Incompressible Fluid Flows, research report, Los Alamos Scientific Laboratory of the University of California, Los Alamos, N.M., 1970.
18. S. V. Patankar, Numerical Prediction of Three-Dimensional Flows, in B. E. Launder (ed.), *Studies in Convection*, pp. 1–78, Academic Press, New York, 1975.
19. O. R. Burggraf, Analytical and Numerical Studies of the Structure of Steady Separated Flows, *J. Fluid Mech.*, vol. 24, pt. 1, pp. 113–151, 1966.
20. D. K. Gartling, Finite Element Analysis of Viscous, Incompressible Fluid Flow, Ph.D. thesis, Univ. of Texas, Austin, 1975.

Requests for reprints should be sent to G. E. Schneider.